

## Simulations of antenna response for the Radio Detector of the Pierre Auger Observatory

---

Ugo Giaccari<sup>a</sup> on behalf of the Pierre Auger Collaboration<sup>b</sup>

<sup>a</sup>*Department of Astrophysics/IMAPP, Radboud University,  
PO Box 9010, NL-6500 GL Nijmegen, The Netherlands*

<sup>b</sup>*Observatorio Pierre Auger, Av. San Martín Norte 304, 5613 Malargüe, Argentina*

*E-mail: [u.giaccari@astro.ru.nl](mailto:u.giaccari@astro.ru.nl), [spokespersons@auger.org](mailto:spokespersons@auger.org)*

After more than 15 years of successful operation, the Pierre Auger Observatory is currently undergoing a major upgrade called AugerPrime. The aim is to study the mass composition of ultra-high-energy cosmic rays. Part of the upgrade program consists in installing a Short Aperiodic Loaded Loop Antenna (SALLA) atop each of the 1660 water-Cherenkov detectors.

To obtain an absolute calibration for the SALLA, the frequency and directionally dependent antenna response (or vector effective length) must be known. The characteristics of the SALLA depend on various parameters, most prominent is the considered frequency of reception and the antenna geometry. Moreover, the interaction with the structure elements and the presence of the ground has an impact. The measurement of the characteristics of the SALLA is a complex experimental effort. In this view, investigation by numerical antenna simulations provides an important and useful tool. In this contribution, we describe the method used to calculate the vector equivalent length of the SALLA with an advanced and widely used software for antenna simulations like the Numerical Electromagnetics Code (NEC).

*9th International Workshop on Acoustic and Radio EeV Neutrino Detection Activities - ARENA2022  
7-10 June 2022  
Santiago de Compostela, Spain*

## 1. Introduction

The Auger Engineering Radio Array (AERA) [1], as a part of the Pierre Auger Observatory [2], has consistently demonstrated its scientific productivity. With more than 150 autonomous antenna stations spread over 17 km<sup>2</sup>, AERA measures the radio emission from extensive air showers in the frequency range between 30 and 80 MHz. The atmospheric depth of the maximum shower development has been measured with AERA using showers with zenith angle below 55° [3]. Air showers with zenith angles above 60° have a large footprint of the radio emission on the ground and have been also measured with AERA demonstrating the feasibility of the radio technique for highly inclined showers [4].

Based on the AERA success and results, a Radio Detector (RD) [5] is also included in the upgrade program of the Pierre Auger Observatory [6]. A Short Aperiodic Loaded Loop Antenna (SALLA) [7] is going to be installed atop each water-Cherenkov detector to improve the measurements of the highly inclined showers [8]. Each station is equipped with two loop antennas, one oriented parallel to the Earth's magnetic field and the other perpendicular to it. To perform a calibrated measurement of the radio emission the impact of the detector and especially of the antenna needs to be unfolded from the recorded signals. It is necessary to have a good understanding of the detector response, including gains and losses in the signal chain, the directional response of the antennas and dispersion in the system.

The purpose of this paper is to describe the method used to simulate the response of the SALLA in the frequency domain using the Numerical Electromagnetics Code (NEC) modeling software [9], a popular antenna modeling system for wire and surface antennas that simulates the electromagnetic response of antennas and metal structures. Several releases of the NEC software exist, however, the most widely used and distributed is NEC2. For our studies we use 4NEC2 [10] because it has many more options than the other versions.

The vector effective length (VEL) contains the full information on the response of an antenna structure. The VEL is given by ratio of the voltage  $V(\omega)$  to an incoming electric field  $\vec{E}(\omega, \theta, \phi)$  for a given direction  $(\theta, \phi)$ . The aim of this contribution is to calculate the VEL of the SALLA from the simulations obtained with the NEC2 program. In NEC2, a table of the vector values of the electric field is generated for each frequency and is independent of the distance to the origin. Thus the method described here is valid only for far field conditions. Hereafter the origin of the coordinate system is located at ground level below the centre of the antenna structure, the ground is in the XY plane and the Z axis represents the height over the ground with the positive X axis pointing the East. The  $\theta$  angle is measured between the positive Z semi-axis and the ground plane XY, the  $\phi$  is measured between the positive X semi-axis and the YZ plane. It is convenient to express the complex value of  $\vec{H}(\omega, \theta, \phi)$  for the two directions  $\hat{e}_\theta$  and  $\hat{e}_\phi$ :  $\vec{H}(\omega, \theta, \phi) = H_\theta(\omega, \theta, \phi) \hat{e}_\theta + H_\phi(\omega, \theta, \phi) \hat{e}_\phi$ , where  $H_\phi$  and  $H_\theta$  are the horizontal and meridional VEL components.

## 2. Antenna characteristics

The antenna type chosen to detect the radio emission from air showers in the frequency range between 30 to 80 MHz is a short aperiodic loaded loop antenna (SALLA). This type of antenna has been developed to provide a minimal design that fulfills the need for both, ultra-wideband

sensitivity, and low costs for production and maintenance of the antenna in a large-scale radio detector. The compact structure of the SALLA makes the antenna robust and easy to manufacture. The SALLA realizes a Beverage antenna as a dipole loop of 1.2 m diameter and with a tube's width of 1 cm radius [7]. A resistor load is included within the antenna structure to give a specific shape to the directivity. In the case of the SALLA a resistance of  $450 \Omega$  connects the ends of the dipole arms at the bottom of the antenna. The antenna is read out at the top which is also the position of the Low-Noise Amplifier (LNA). While signals coming from above will induce a current directly at the input of the amplifier, the reception from directions below the antenna is strongly suppressed as the captured power is primarily consumed within the ohmic resistor rather than amplified by the LNA. The resulting suppression of sensitivity towards the ground reduces the dependence of the antenna on ground conditions but its influence is still an important parameter for the calculation of the VEL components. There are different ways for modeling the ground in 4NEC2, here we use the real ground option (aka Sommerfeld-Norton) which gives us the highest accuracy of results for antenna models above the soil. For this contribution we use the ground properties of the AERA-site [7], the relative permittivity is 5.5 and the conductivity is 0.0014 S/m.

For each of the two loop antennas, we have produced a NEC geometry file describing the antenna and its environment. We have used a voltage source at the terminal of the first antenna loop and a load equivalent to the input impedance of the LNA on the other antenna terminal in order to calculate the electric field of the first loop. For the second antenna loop we have swapped the voltage source and the load and repeated the operation to calculate the electric field of the second loop. The electric field values simulated with 4NEC2 have been combined with the scattering parameters of the LNA for obtaining the VEL of the SALLA at the LNA output. For lack of space we will only show the results of the simulations for the antenna loop along the XZ plane perpendicular to the Earth's magnetic field.

### **3. Salla model in 4NEC2**

In the 4NEC2 geometry file it's not possible to model a circular loop antenna like the SALLA, for this reason we have implemented and compared three different models made by of a regular polygon inscribed to a circle with a 1.2 m diameter. The three models are an octagon, a 16-sided and a 32-sided polygon. All these models have the same tube's width of 1 cm radius and satisfy the NEC requirement about the ratio between the length of the segment and the wavelength. We have compared the simulated responses for three models considering the antenna alone above the same soil. In Figure 1(a) and Figure 1(b) there are the two VEL components for two fixed directions, indicated at the top of each plot, as a function of the frequency. The two directions in azimuth correspond to the region of maximum sensitivity for the meridional and horizontal VEL components. The models corresponding to the 16-sided and 32-sided polygons give us similar results while there are some differences with the octagon model. Making the average over all the possible directions above the ground, we see that the difference are below  $\sim 1.5\%$  for the 16-sided and 32-sided models and at the order of  $\sim 5\%$  for the octagon and the 32-sided polygon. We chose the 32-sided polygon model for simulating the response of the SALLA.

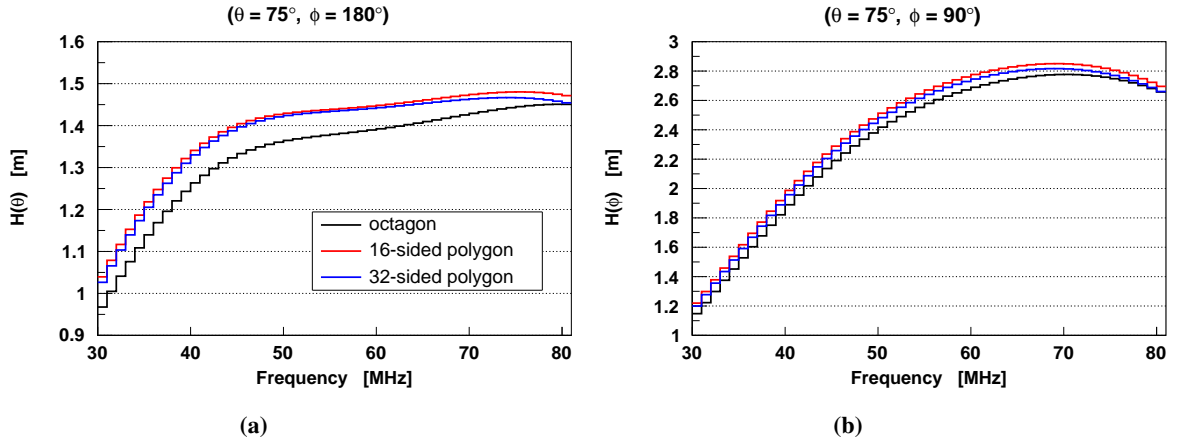


**Figure 1:** Figure1(a) and Figure1(b) show the meridional and horizontal VEL components for two fixed directions, indicated at the top of each plot, as a function of the frequency for the three models describing the SALLA (see text).

#### 4. Surface Detector Station at the Pierre Auger Observatory

The goal of this section is to assess the influence of the complete structure below the SALLA on the radiation pattern compared to the pattern of the antenna alone above the same soil. To achieve this we have simulated the response of the SALLA and added each time each individual component of the Surface Detector Station to investigate its effect on the antenna response. The complete design of Surface Detector Station has been considered in this work and implemented within the NEC framework. In Figure 2 there is the 3D visualization for the Surface Detector Station. At the bottom the water-Cherenkov Detector and on its top the other components such as the Scintillator Detector, the solar panels, the communications antenna and the supporting structure for the scintillator detector and the SALLA. The mast, the cables and the frame influence the antenna response, in particular the mast has dominant vertical dimension and will therefore couple with the meridional polarized component of the VEL field. The LNA is located at the top of the antenna at an altitude of 5 m in a plastic housing not in the center of the system of reference. From the LNA the signal goes through two coaxial cables inside a fiberglass mast to the digitizer. Each cable has a diameter of 0.2 cm considering only the metal shielding part. Note that NEC2 has limitations when modeling structures very close to each other, we model the two coaxial cables

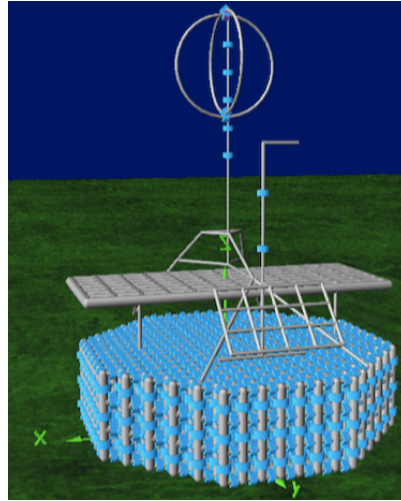


**Figure 2:** 3D visualization of the SALLA and the complete Surface Detector Station of the Pierre Auger Observatory implemented in 4NEC2.

with one conductor with twice the circumference, one cable (wire) with radius 0.2 cm. Below the fiberglass mast the radius is 1.5 cm down to the antenna frame. The mere use of the fiberglass mast

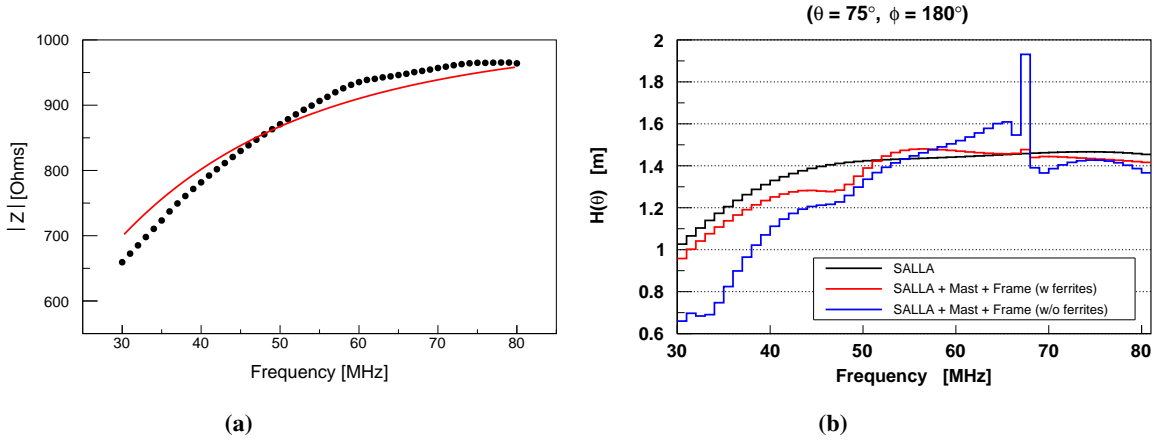


**Figure 3:** 3(a) the black dots indicate the measured amplitude of the ferrite core impedance. The red line represents the best-fit line with a RLC parallel circuit. 3(b) shows the simulated meridional VEL component as a function of the frequency for the antenna only (black line), the antenna plus the mast and the frame with (red line) and without (blue line) the ferrite cores.

is not enough for decoupling the mast-cables influence. For the decoupling of the antenna response we have used 5 ferrite cores with two windings [11]. The main reason is to ensure that the coaxial cable's shield does not become part of the antenna system and will radiate unintentionally. It is important to reproduce the impedance of the ferrite cores in the simulations of the antenna response. Given NEC2 properties we have implemented a description of the ferrite cores with a RLC parallel circuit with a resistor of  $966 \Omega$ , an inductor of  $5.4 \mu H$  and a capacitor of  $0.7 \text{ pF}$ . Anyway it is hard to find a good parametrization of the measured amplitude and phase of the impedance at the same time using a RLC parallel model. We notice that the amplitude has a major impact on the decoupling of the antenna with respect the phase, for this reason the basic components of the RLC parallel circuit have been obtained from fitting the amplitude of the impedance, see Figure 3(a). To have an idea of the importance of the decoupling made with the ferrite cores, in Figure 3(b) there is the simulated meridional VEL component,  $H(\theta)$ , as a function of the frequency for the antenna only (black line), for the antenna plus the mast and the frame with (red line) and without (blue line) the ferrite cores. The decoupling effect of the ferrite cores that reduce drastically re-radiation from the mast and the frame is clearly visible. With the decoupling the influence of the mast-cables is significantly reduced and the relative differences with the only SALLA response are up to the  $\sim 6\%$  level, the major effect is around 40-50 MHz. Also the positions of the ferrite cores are important in the decoupling of the antenna, using NEC simulations their positions have been optimized to reduce the re-radiation from the mast and the cables. The solar panel of the Surface Detector Station is modeled as a grid wire with a  $0.25 \times 0.3 \text{ m}^2$  grid size and with a radius of 15 mm for each grid wire. For the communications antenna we have used wires with a radius of 5 mm and for its mast a radius of 15 mm. In Figures 4(a) and 4(b) it is possible to see the influence of the solar panel and of the communications antenna (blue line) compared to the SALLA alone and the SALLA with the mast and the frame. The solar panel has a mild impact on the VEL components,

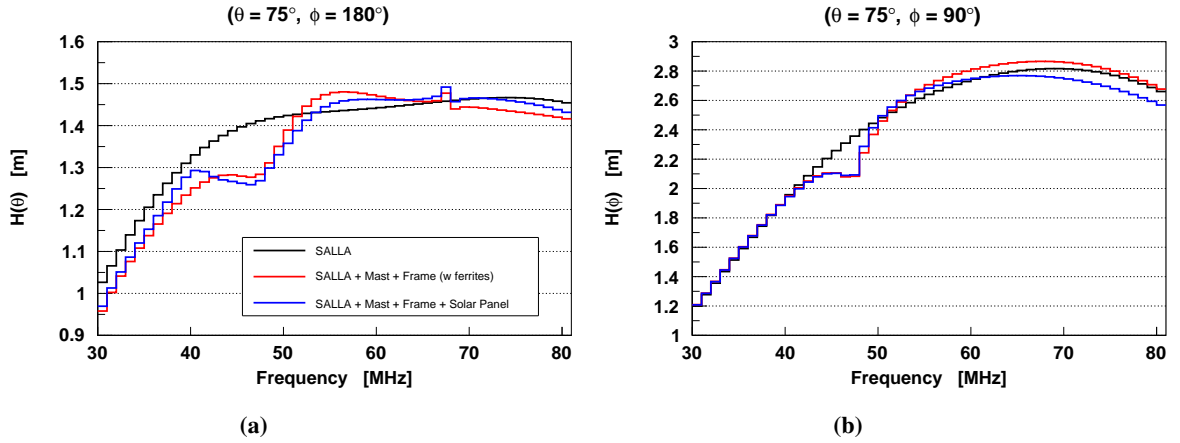


**Figure 4:** Figures 4(a) and 4(b) show the simulated SALLA response alone (black line), the SALLA plus the mast, the cables with (blue line) and without (red line) the solar panel.

on average over all the directions the differences are of the order of  $\sim 3\%$ . The structure of Surface Scintillator Detector (SSD) of the Surface Detector Station is an electrically large object with respect the other components of the Surface Detector Station. For the 4NEC2 simulations we have used a thicker radius for the wire of this structure. In this way we can account for reflections to the antenna loops. The structure of the SSD is modeled as a grid with  $0.2 \times 0.3 \text{ m}^2$  grid size and a radius of 60 mm for the grid wires. In Figures 5(a) and 5(b) it is possible to see the effect of the structure of the SSD on the SALLA response for the two chosen specific directions, on average the relative differences are of the order of few % at all frequencies for both VEL components but around  $\sim 30 \text{ MHz}$  are around  $\sim 15\%$  for the horizontal VEL component.

The water-Cherenkov Detector (WCD) is a difficult object to model as NEC cannot simulate dielectric volumetric objects. Modeling the WCD as a metal wire grid for surface currents may show more pattern distortion than will happen in real world, for this reason we implement in NEC an object with the same reflection properties of pure water with a square resistance of 47 Ohms. The

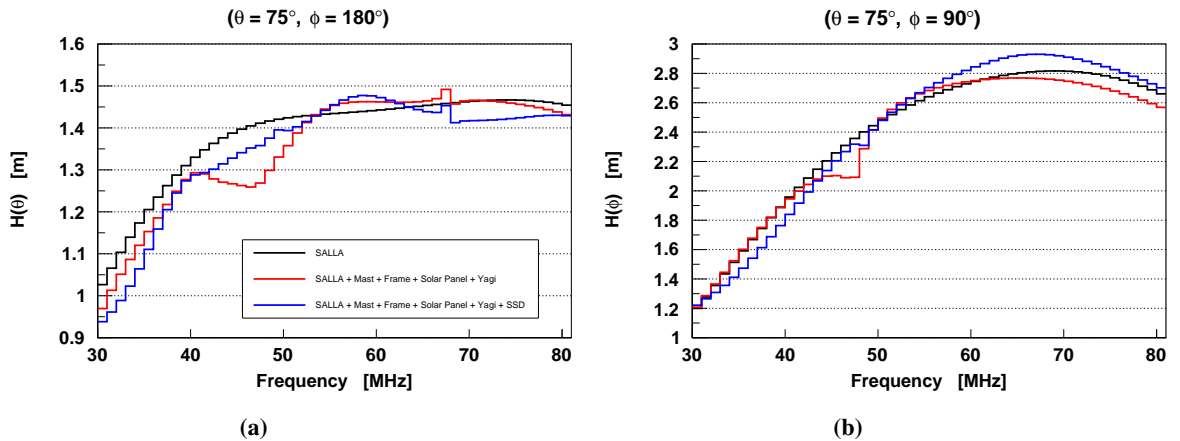


**Figure 5:** Simulated VEL components with the SALLA alone (black line), considering the mast the frame (red line) and also including the solar panel and communications antenna (blue line).

shape of WCD in our model is an octagon with the top/bottom grid size of  $0.2 \times 0.2 \text{ m}^2$  and the side with  $0.2 \times 0.3 \text{ m}^2$  grid size. In Figure 2 there is the 3D model implementation with 4NEC2 with the full Surface Detector Station and the WCD at the bottom. NEC2 requirements with the real ground option do not allow wires touching the soil, for this reason wires need to be above ground. The bottom of the WCD is therefore 0.2 m above ground. On average over all the directions the effect of WCD upon the SALLA patterns are within 5% for the meridional VEL component and between 5% and 15% for the horizontal one. We have also tested a different model of the WCD with an empty box with the same square resistance of 47 Ohms and notice that the SALLA response do not depend significantly on the shape of the WCD.

In Figure 6 we show the SALLA response for a set of three frequencies as a function of the local angles  $(\theta, \phi)$ . For the low frequencies, the SALLA is more sensitive to zenith angles below  $30\text{-}40^\circ$ . At higher frequencies, a side-lobe pattern evolves with up to two lobes at the highest frequencies with more sensitivities for high zenith angle values in the range between  $\sim 70^\circ$  and  $80^\circ$ . We show also in Figure 7 the group delay as a function of the frequency for a set of directions for the meridional (top row) and horizontal VEL component (bottom row).

## 5. Conclusion

We have described a method used to simulate the vector equivalent length of the SALLA with a widely used software for antenna simulations (4NEC2). All the components of the Surface Detector Station of the Pierre Auger Observatory have been included in the calculation and their effect have been studied. The response showed in this contribution includes also the LNA scattering parameters. The vector effective length obtained in this study will be compared with the on-site measurements of the antenna response scheduled for the next months.

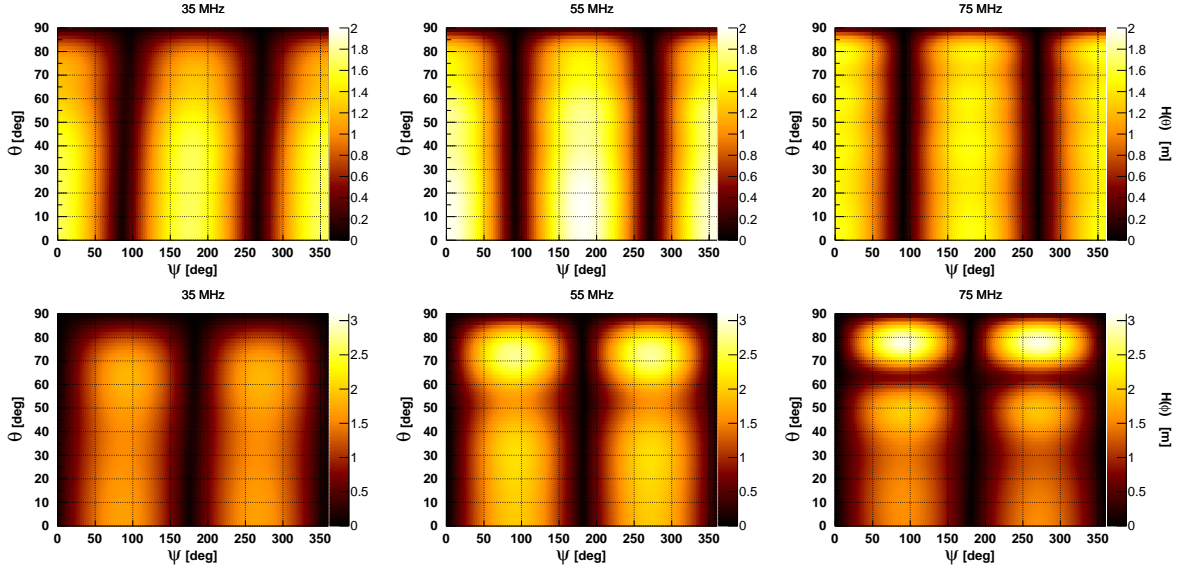


**Figure 6:** On the top row there are the simulated meridional VEL components as a function of the local angles  $(\theta, \phi)$  for 35 MHz, 55 MHz and 75 MHz, on the bottom the horizontal VEL components for the same set of frequencies.

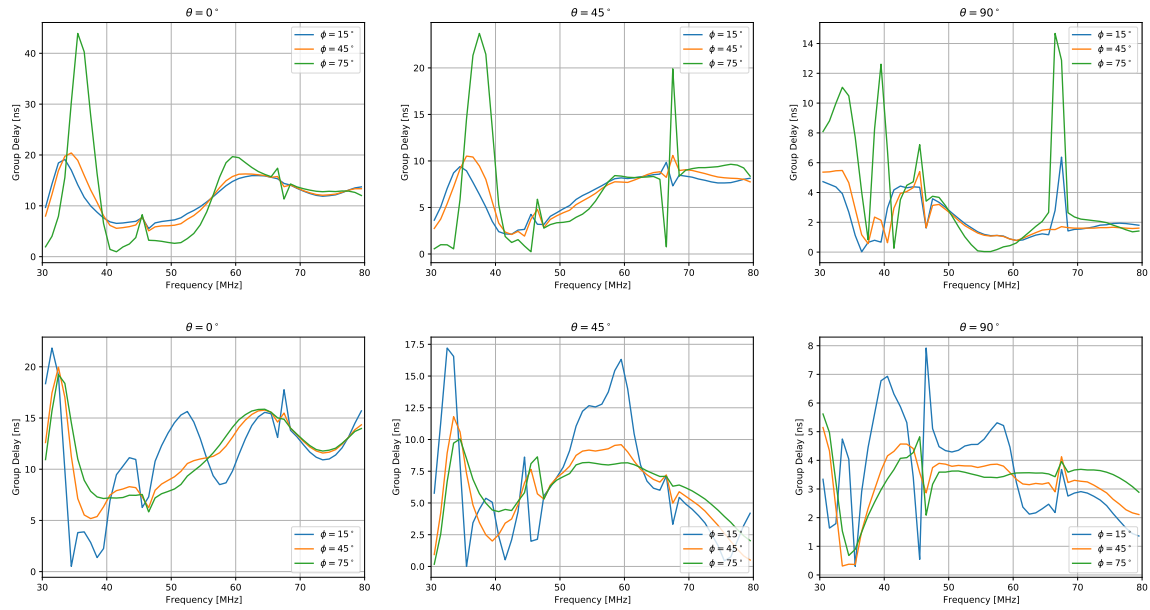


**Figure 7:** On the top and on the bottom the group delay for the meridional and horizontal VEL components for a set of directions.

## References

- [1] E. M. Holt on behalf of The Pierre Auger Collaboration, PoS(ICRC2017)492
- [2] A. Aab, et al., Nucl. Instrum. Meth. A 798 (2015) 172–213, [1502.01323].
- [3] B. Pont on behalf of The Pierre Auger Collaboration, PoS(ICRC2021)387
- [4] A. Aab, et al., JCAP10(2018)026
- [5] J. Hörandel for The Pierre Auger Collaboration, EPJ Web of Conferences 210, 06005 (2019)
- [6] A. Aab, et al., arXiv [1604.03637][astro-ph.IM]
- [7] P. Abreu, et al., JINST 7 (2012) P10011.
- [8] F. Schlüter on behalf of The Pierre Auger Collaboration, PoS(ICRC2021)262
- [9] G. Burke, A. Poggio, J. Logan, J. Rockway, “NEC - Numerical Electromagnetics code for Antennas and Scattering,” Antennas and Propagation Society International Symposium, 1979, 17:147-150
- [10] <https://www.qsl.net/4nec2/>
- [11] <https://www.fair-rite.com/product/round-cable-snap-its-431167281>